

NANOFRACTOGRAPHY OF COMPOSITION B FRACTURE SURFACES WITH AFM

Y. D. Lanzerotti*
U. S. Army ARDEC
Picatinny Arsenal, NJ 07806-5000

J. Sharma
Naval Surface Warfare Center, Carderock Division
West Bethesda MD 20817-5700

R. W. Armstrong
U. Maryland, Dept. Mechanical Engineering
College Park, MD 20742

R. L. Mc Kenney and T. R. Krawietz
AFRL-MNME, 2306 Perimeter Rd.
Eglin AFB, FL 34542-5910

ABSTRACT

The characteristics of TNT crystals in the fracture surface of Composition B (a melt-cast composition of RDX, TNT and wax) have been studied using atomic force microscopy (AFM). The sub-microscopic size of the TNT crystal component is revealed by the surface structure that is exhibited after mechanical failure. The failure surfaces are produced by subjecting the material to high acceleration in an ultracentrifuge under conditions in which the shear or tensile strength is exceeded.

AFM examination of the TNT component fracture surface topography reveals that essentially brittle cleavage has occurred across the very finely-spaced columnar grains. The width of the grains varies narrowly in size between $\sim 1 \mu\text{m}$ and $\sim 2 \mu\text{m}$. The height elevations of the inclined and stepped surfaces range in size between $\sim 50 \text{ nm}$ to $\sim 300 \text{ nm}$. Shear-type deformation that has occurred prior to cleavage fracture is evidenced in the lowest magnification images, that is, for the largest AFM scans ($8 \mu\text{m}$ and $13.5 \mu\text{m}$). Specularly cleaved column surfaces alternate with ones containing profuse river patterns identifying the directions of crack growth. The river pattern markings are observed to originate at the boundaries between adjacent columns whereas the average profile angles between adjacent columnar surfaces are within the theoretical limit for dislocations. The smallest, individual, nm-size step heights at the river pattern ledges are smaller than the unit cell dimensions of either allotropic crystal phase of TNT. Such steps, smaller than unit cell dimensions, may relate to the important issue of breaking intramolecular bonds.

1. INTRODUCTION

Energetic materials are of interest for scientific and practical reasons in the extraction (mining) industry, structure demolition, space propulsion, and ordnance. In such applications the materials can be subjected to high, fluctuating, and/or sustained acceleration. The nature of the fracture process of such materials under high acceleration is of particular interest, especially in ordnance and propulsion applications. For example, explosives in projectiles are subjected to setback forces as high as $50,000 g$ ($g = 980.6 \text{ cm/s}^2$) during the gun launch process. These high setback forces can cause fracture and premature ignition of explosives.

Fundamental understanding of the behavior of energetic materials subjected to high acceleration is a key to better practical ordnance designs that solve the problems of abnormal propellant burning and premature ignition of explosives during gun launch. An energetic material will experience a pressure gradient during acceleration in the gun, as well as under g -loading in a laboratory experiment in an ultracentrifuge. The pressure gradient that is experienced by the explosive during acceleration in the gun and under g -loading in the ultracentrifuge is unique and will produce different kinds of behavior and failure than under other material test conditions. This work is particularly relevant to the future development of insensitive energetic materials to be used in devices with higher acceleration.

Because of the general importance of the topic, the mechanical behavior of energetic materials during high acceleration has been studied by using an ultracentrifuge (Lanzerotti and Sharma, 1981; Lanzerotti et al., 1993, 1996, 1997; Meisel et al., 2000) and appropriate diagnostic techniques. This

Report Documentation Page				Form Approved OMB No. 0704-0188	
Public reporting burden for the collection of information is estimated to average 1 hour per response, including the time for reviewing instructions, searching existing data sources, gathering and maintaining the data needed, and completing and reviewing the collection of information. Send comments regarding this burden estimate or any other aspect of this collection of information, including suggestions for reducing this burden, to Washington Headquarters Services, Directorate for Information Operations and Reports, 1215 Jefferson Davis Highway, Suite 1204, Arlington VA 22202-4302. Respondents should be aware that notwithstanding any other provision of law, no person shall be subject to a penalty for failing to comply with a collection of information if it does not display a currently valid OMB control number.					
1. REPORT DATE 00 DEC 2004		2. REPORT TYPE N/A		3. DATES COVERED -	
4. TITLE AND SUBTITLE Nanofractography Of Composition B Fracture Surfaces With Afm				5a. CONTRACT NUMBER	
				5b. GRANT NUMBER	
				5c. PROGRAM ELEMENT NUMBER	
6. AUTHOR(S)				5d. PROJECT NUMBER	
				5e. TASK NUMBER	
				5f. WORK UNIT NUMBER	
7. PERFORMING ORGANIZATION NAME(S) AND ADDRESS(ES) U. S. Army ARDEC Picatinny Arsenal, NJ 07806-5000; Naval Surface Warfare Center, Carderock Division West Bethesda MD 20817-5700				8. PERFORMING ORGANIZATION REPORT NUMBER	
9. SPONSORING/MONITORING AGENCY NAME(S) AND ADDRESS(ES)				10. SPONSOR/MONITOR'S ACRONYM(S)	
				11. SPONSOR/MONITOR'S REPORT NUMBER(S)	
12. DISTRIBUTION/AVAILABILITY STATEMENT Approved for public release, distribution unlimited					
13. SUPPLEMENTARY NOTES See also ADM001736, Proceedings for the Army Science Conference (24th) Held on 29 November - 2 December 2005 in Orlando, Florida. , The original document contains color images.					
14. ABSTRACT					
15. SUBJECT TERMS					
16. SECURITY CLASSIFICATION OF:			17. LIMITATION OF ABSTRACT UU	18. NUMBER OF PAGES 8	19a. NAME OF RESPONSIBLE PERSON
a. REPORT unclassified	b. ABSTRACT unclassified	c. THIS PAGE unclassified			

includes study of the characteristics of the fracture surfaces of the materials. Several important new discoveries have been made in the course of studies of the topography of the fracture surfaces of energetic materials using fractal (Lanzerotti et al., 1997) and self-affine (Meisel et al., 2000) data analysis techniques. Through diamond stylus profilometer measurement and fractal analysis of spatial power spectra of fracture surface profiles of melt-cast TNT and TNT formulations in the spatial frequency range of 1 mm^{-1} to 10 mm^{-1} (spatial wavelengths 1 mm to 0.1 mm), predominantly deterministic intergranular failure has been found to occur when the shear or tensile strength of the explosive is exceeded (Lanzerotti et al., 1993). AFM topography measurements and power spectral analysis of the data in the spatial frequency range of $1 \mu\text{m}^{-1}$ to $10^2 \mu\text{m}^{-1}$ (spatial wavelengths 1 μm to 0.01 μm) also demonstrate deterministic fracture (Lanzerotti et al., 1997).

Curved reference surfaces are used to perform height correlation function-based self-affine fractal analysis of textures in cases that cannot be analyzed with respect to flat reference surfaces. Employing curved local reference surfaces, self-affine fractal analysis has been used to characterize scaling on curved TNT fracture surfaces (Meisel et al., 2000). SEM studies of the pro-eutectic RDX crystal constituents in the fracture surface of Composition B have been performed and reported previously by others (Smith and Thorpe, 1973) but attempts to observe details in the fracture surfaces of the eutectic TNT constituent have been described previously as too fine to be resolved.

Previously, RDX crystals have been grown during high acceleration (200,000 g) in the ultracentrifuge (Lanzerotti et al., 1996). AFM studies of these RDX crystals have shown that they have fewer defects than RDX crystals grown at 1 g (Sharma et al., 2001).

2. EXPERIMENTAL

A Beckman ultracentrifuge model L8-80 with a swinging bucket rotor model SW 60 Ti is used to rotate the sample under study up to 60,000 rpm (about 500,000 g). The distance of the specimen from the axis of rotation, between 6 and 12 cm, can be chosen as a variable.

Samples are prepared as follows. Cylindrical polycrystalline plugs of explosive are prepared by pouring about one-half gram of the material into 9-mm internal diameter polycarbonate or steel tubes and

allowing the material to crystallize. The open-ended sample tube is then joined to a short, closed-end polycarbonate centrifuge tube. The as-cast surface of the explosive faces away from the axis of the rotation.

The sample experiences a time rate of change of the acceleration up to a maximum acceleration. The sample then remains at this maximum acceleration for an interval such that for each run there is a combined total elapsed time of five minutes. The sample then decelerates smoothly to zero acceleration. The initial maximum acceleration is less than the fracture acceleration for the material. The maximum acceleration for the sample is then increased systematically in each successive five-minute run. The sample fractures when the shear or tensile strength of the material is exceeded. At this time, particles break loose from the surface exposed to the acceleration and transfer to the closed-end tube. A hemispherical fracture surface is formed on the sample.

In this present study, a Nanoscope III atomic force microscope was used to measure the topography of the Composition B fracture surface. The oxide sharpened silicon nitride cantilevers have tips with a radius of about 10 nm. Long thin cantilevers with a force of about 20 nN were used.

2. RESULTS

Composition B is a melt-cast composition of 59% cyclotrimethylenetrinitramine (RDX), 40% TNT (trinitrotoluene) and 1% wax. TNT melts at 80.9°C (Dobratz and Crawford, p. 19-143, 1985). RDX melts with decomposition at 205°C (Dobratz and Crawford, p. 19-131, 1985). Composition B is cast as a slurry of solid RDX in molten TNT (Smith and Thorpe, 1973). RDX dissolves in molten TNT; the eutectic is 4.16% RDX at 79°C (Federoff and Sheffield, 1966). Microscopical hot stage observations have been reported for RDX/TNT mixtures (Williamson, 1958). The minor RDX constituent of the eutectic composition was observed to form as particles between the lath-like, or now-termed columnar, crystals of the major TNT eutectic constituent.

Scanning electron microscopy (SEM) studies of the fracture surface of Composition B have revealed the characteristics of the RDX fracture surfaces (Smith and Thorpe, 1973). The RDX crystals range in size from $\sim 100 \mu\text{m}$ to $\sim 1,000 \mu\text{m}$ as specified (Lanzerotti, et al., 1993). Fracture surfaces of RDX crystals and “river patterns” (Hull, 1999) showing direction of crack growth have been observed using SEM techniques (Smith and Thorpe, 1973).

SEM attempts to view the fine surface detail of TNT in the Composition B fracture surface were unsuccessful (Smith and Thorpe, 1973). Although the original work was carried out some time ago, the characteristics of TNT crystals remain a subject of investigation in melt-cast TNT formulations that are filled with a large percentage of RDX.

The size of TNT crystals in a Composition B fracture surface has been determined in this work by analyzing with an AFM the surface structure that is exhibited after mechanical failure of the Composition B at high acceleration in an ultracentrifuge. The sample of melt-cast Composition B used for the AFM studies fractured at 46,000 g at 25°C. AFM examination of the topography of the fracture surface of the Composition B reveals fracture that occurs across columnar grains of the TNT. An AFM scan of

TNT columnar grains in the Composition B fracture surface is shown in Figure 1. The AFM scan sizes were increased in steps from 2 μm to 13.6 μm with the maximum scan size ultimately limited by the curvature of the fracture surface.

Each three-dimensional AFM scan consists of 512 uniformly spaced height profiles. For the AFM scan discussed here, the horizontal spacing of the successive profiles is the 4.0 μm scan width divided by 511 spaces or 8 nm. Each height profile is composed of 512 uniformly spaced (8 nm) height values. The first data point is the lower left hand corner of a scan (e.g., Fig. 1). The second profile then begins above the first data point. The last point in the final profile corresponds to the upper right hand corner data point.

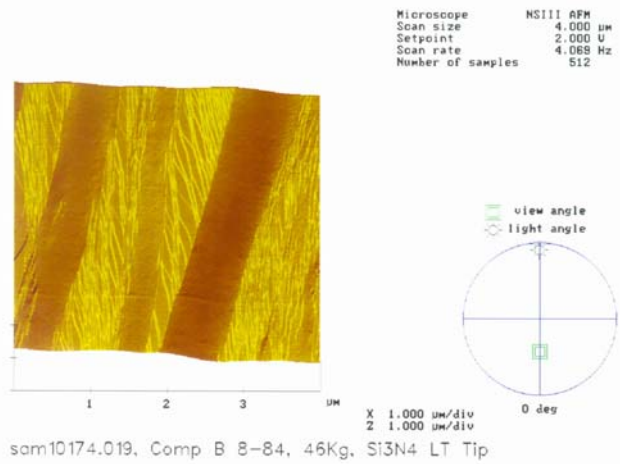


Figure 1. 4.0 μm AFM scan of TNT columnar grains in Composition B fracture surface

The measured width and height of the TNT columnar grains are given as a function of the AFM scan sizes in Table I. The data were measured from the first profile of each TNT AFM scan. The compiled data in Table I show that the width of the columnar TNT grains ranges from $\sim 1 \mu\text{m}$ to $\sim 2 \mu\text{m}$. The height of the columnar TNT grains ranges in size from $\sim 50 \text{ nm}$ to $\sim 300 \text{ nm}$. To the best of our knowledge, values of these quantities for TNT in Composition B

have not been reported before and were said to be unsuccessfully looked for (Smith and Thorpe, 1973). The microstructure of the matrix of TNT is normally one of highly oriented columnar grains (Smith and Thorpe, 1973). Therefore, the results of Table I suggest that the AFM scans are measurements of the fracture across TNT columnar grains in Composition B.

Table I. TNT columnar grains in AFM scans

Scan size (μm)	TNT columnar grains	Width (μm)	Height (nm)
2.0	2	1	60-300
4.0	4	1	50-300
8.0	5	1-2	100-300
13.6	7	1-2	100-300

The fracture surface microstructure of the TNT grains of Figure 1 show flat TNT columns alternating with TNT columns containing river patterns. The river patterns provide information on

the direction of the crack growth of the fracture surface (Hull, 1999). In Figure 1, the crack growth is from the top to the bottom of the Figure.

The 512 height points from profile 99 of the 4 μm scan of TNT are broken into five segments of 100 points (800 nm lengths) each. These segments are shown in Figures 2a - 2e. The steps in the river patterns are evident in these figures. The steps in the river patterns are a few nanometers in depth. From the profile measurements, the slope of the large facet in Figure 2a is $\sim -11^\circ$ and the individual stepped risers

are < 1 nm in height. The first inclined facet near to the Figure 2b origin is at $\sim 11^\circ$, terminating in step risers of $\sim 1\text{-}3$ nm; and, likewise, the slopes in Figure 2c are $\sim -11^\circ$ and $\sim 7^\circ$. These angles are within the theoretical limit for dislocations. The small angular inclinations between adjacent average fracture facet orientations are exaggerated, of course, by the vertical height sensitivity of the AFM technique/method.

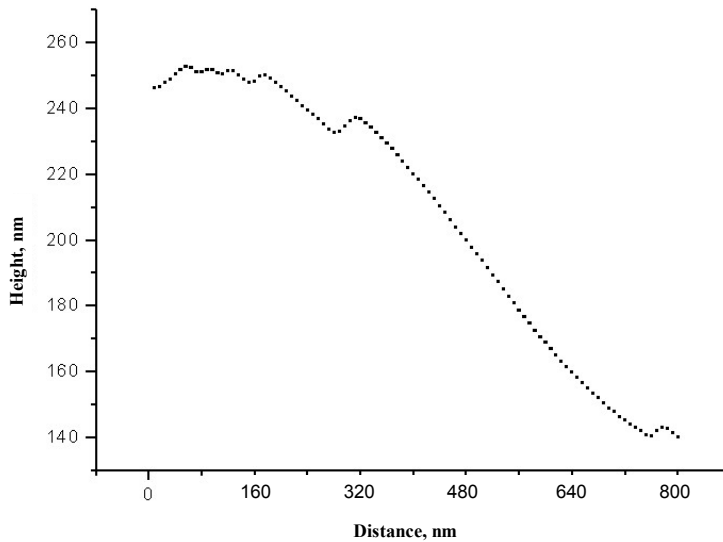


Figure 2a. Composition B Fracture Surface, Profile 99, 4.0 μm Scan Section

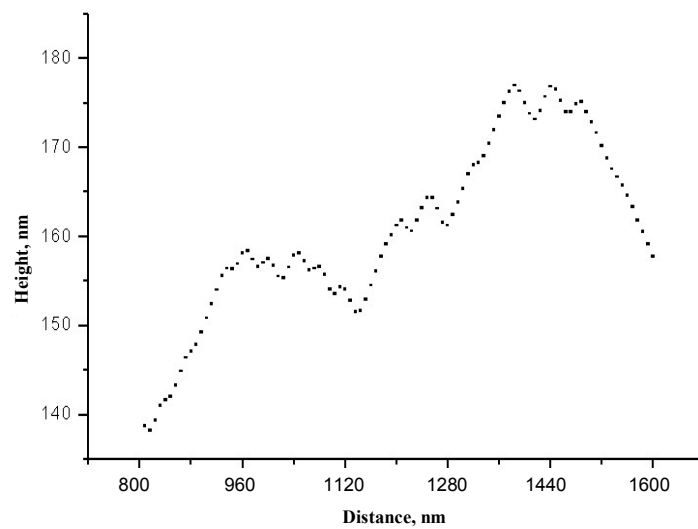


Figure 2b. Composition B Fracture Surface, Profile 99, 4.0 μm Scan Section

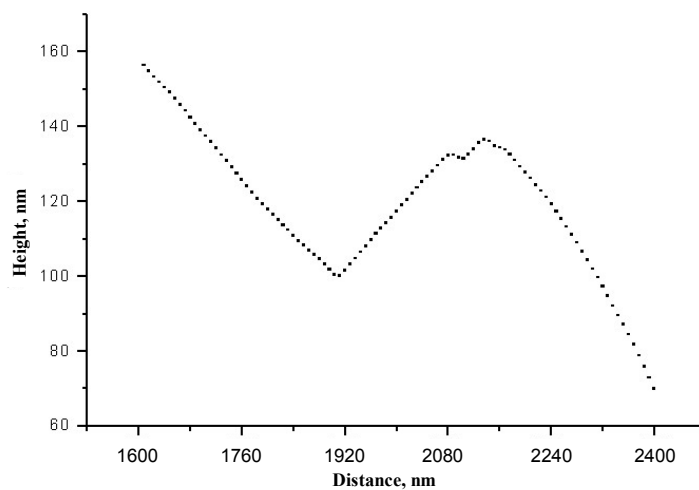


Figure 2c. Composition B Fracture Surface, Profile 99, 4.0 μm Scan Section

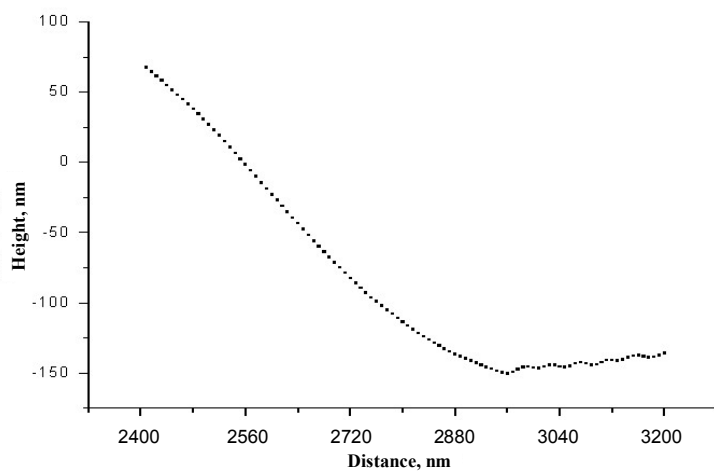


Figure 2d. Composition B Fracture Surface, Profile 99, 4.0 μm Scan Section

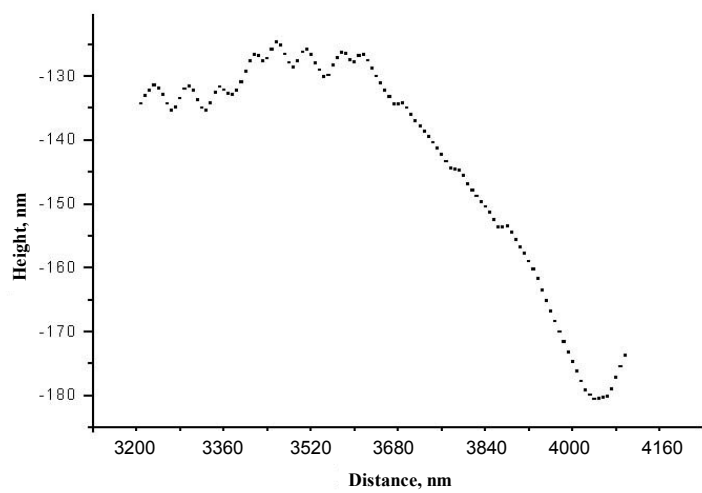


Figure 2e. Composition B Fracture Surface, Profile 99, 4.0 μm Scan Section

4. DISCUSSION

Several factors have been considered in explaining, in the first place, why the TNT columnar grain morphology should be so finely spaced and, then, why the cleavage morphology should occur on an even finer scale. One promising possibility relates to the complication of there being two kinds of TNT molecules, designated A and B, occurring within several monoclinic or orthorhombic unit cell structures (Miller and Garroway, 2001). Also, the monoclinic form(s), mostly assumed to be the ones present at low temperature, are known to exhibit copious twinning across the (100) plane with extension in the [001] direction, forming a re-entrant corner at the common (100) twin interface. The half-unit cell structure on either side of the (100) interface forms the new unit cell structure, apparently, of the orthorhombic lattice specification (Gallagher et al., 1997; Gallagher, et al., 2003). Such unit cell structures, each involving eight molecule positions, have representative lattice parameters of ~ 0.6 , ~ 1.5 , and $\sim 2.0 - 2.1$ nm lengths. No identification of potential cleavage planes are given in Miller and Garroway (Miller and Garroway, 2001). TNT is known to be relatively ductile compared to the other listed energetic materials and shear deformation before fracture is observed in the largest AFM scans (not shown here).

The preferred [001], or c-axis, growth of TNT crystals has been reported even within high concentration RDX/TNT castings (Chick, et al., 1970). A promising explanation for occurrence of the long columnar TNT crystals relates to expectation of preferred monoclinic crystal growth along the [001] direction in accordance with a molecular re-entrant corner process of molecular attachment (Seidensticker and Hamilton, 1963). Alternatively, such preferred columnar growth may relate to allotropic connection with the epitaxially related orthorhombic structure. Further research is needed on this aspect of the present observations. Such crystallographic connection also relates to the observation in Figure 1 that the river pattern markings often seem to originate at the smooth/stepped border between presumed adjacent crystal morphologies, also occurring in repetitive pattern. The boundary between the cleaved TNT columns and the TNT columns containing river patterns is the (100) plane.

Lastly, we note that the smallest individual step heights measured at the river pattern ledges are smaller than the unit cell dimensions that are given. Such observation was made for cleavage step heights on shocked RDX crystals (Sharma, et al., 2001).

Here, we suggest that such smaller step heights might be accounted for by partial dislocation Burgers vectors that penetrate the cleavage surface or by only a component of the actual unit dislocation Burgers vector being normal to the cleavage plane. The observation is important in understanding the influence of mechanical forces on the detonation of energetic materials because such liberated energy comes from intramolecular decomposition, not from fracturing of the weaker molecular crystal bonds. Thus, observation of a nanofractured cleavage structure gives indication that such fracturing relates to the length scale of individual molecules being separated from one another, perhaps, in certain cases, in association with the possible breaking even of individual intramolecular bonds.

5.0 ACKNOWLEDGMENTS

We thank Dr. S.A. Mogren, Columbia, MD for assistance in obtaining the AFM scans, and Wayne Richards, AFRL-MNME, Elgin AFB, Florida, for theoretical modeling calculations.

6.0 REFERENCES

- Chick, M. C., Connick W. and Thorpe, B.W., 1970: Microscope Observations of TNT Crystallization, *J. Crystal Growth*, **7**, 317-325.
- Dobratz, B. M. and Crawford, P. C., 1985: LLNL Explosives Handbook, Properties of Chemical Explosives and Explosive Simulants, UCRL-52997 Change 2.
- Federoff, B. T. and Sheffield, O. C., 1966: Encyclopedia of Explosives and Related Items, PATR 2700, **3**, (Picatinny Arsenal, Dover, NJ) p. 615.
- Gallagher, H. G., Roberts, K. J., Sherwood, J. N. and Smith, L.A., 1997: A Theoretical Examination of the Molecular Packing, Intermolecular Bonding and Crystal Morphology of 2,4,6 - Trinitrotoluene in Relation to Polymorphic Structural Stability, *J. Mater. Chem.*, **7**(2), 229-235.
- Gallagher, H. G., Vrcelj, R. M. and Thorpe, B. W., 2003: The Crystal Growth and Perfection of 2,4,6 Trinitrotoluene, *J. Crystal Growth*, **250**, 317-325.
- Hull, D., 1999: Fractography: Observing, Measuring and Interpreting Fracture Surface Topography, (Cambridge U.), p. 93.
- Lanzerotti, Y. and Sharma, J., 1981: Brittle Behavior of Explosives During High Acceleration, *Appl. Phys. Lett.*, **39**, 455-457.
- Lanzerotti, Y., Pinto, J., Wolfe, A. and Thomson, D.

- J., 1993: Fracture Surface Topography of TNT, Composition B and Octol, Proc. Tenth International Detonation Symposium, (Office of Naval Research), 190-198.
- Lanzerotti, Y., Autera, J., Pinto, J. and Sharma, J., 1996: Crystal Growth of Energetic Materials During High Acceleration, *Mat. Res. Soc. Proc.*, **418**, 73-78.
- Lanzerotti, Y., Meisel, L. V., Johnson, M. A., Wolfe, A. and Thomson, D. J., 1997: Fracture Surface Topography of Energetic Materials During High Acceleration, *Mat. Res. Soc. Proc.*, **466**, 179-184.
- Meisel, L. V., Scanlon, R. D., Johnson, M.A. and Lanzerotti, Y., 2000: Fracture Surface Topography of Energetic Materials During High Acceleration, *Mat. Res. Soc. Proc.*, **578**, 363-367.
- Miller, G. R. and Garroway, A. N., 2001: A Review of the Crystal Structures of Common Explosives, Part I: RDX, HMX, TNT, PETN, and Tetryl, Naval Research Laboratory Report NRL/MR/6120-01-8585, 10-16.
- Seidensticker, R. G. and Hamilton, D. R., 1963: Growth Mechanisms in Germanium Dendrites: Three Twin Dendrites; Experiments on and Models for the Entire Interface, *J. Appl. Phys.*, **34**, 3113-3119.
- Sharma, J., Coffey, C. S., Armstrong, R. W., Elban, W. L. and Lanzerotti, Y., 2001: AFM Observations of Growth Sector Structure on a Cleaved RDX Crystal, *Chemical Physics (Russian)*, **20**, 50-54.
- Sharma, J., Armstrong, R. W., Elban, W. L., Coffey, C. S. and Sandusky, H. W., 2001: Nanofractography of Shocked RDX Explosive Crystals With Atomic Force Microscopy, *Appl. Phys. Lett.*, **78**, 457-459.
- Smith, D. L., and Thorpe, R. W., 1973: Fracture in the High Explosive RDX/TNT, *J. Mat. Sci.*, **8**, 757-759.
- Williamson, W. O., 1958: Microscopical Studies of the System RDX and TNT, *J. Appl. Chem.*, **8**, 646-651.